

## INFLUENCE OF THE INTERNALS ORIENTATION ON THE HYDRODYNAMICS IN GAS-SOLID BUBBLING FLUIDIZED BEDS

Frank Schillinger<sup>1</sup>, Simon Maurer<sup>1</sup>, Evert C. Wagner<sup>2</sup>, Serge M.A. Biollaz<sup>1</sup>, J. Ruud van Ommen<sup>2</sup>, Robert F. Mudde<sup>2</sup>, Tilman J. Schildhauer<sup>1\*</sup>

<sup>1</sup>Paul Scherrer Institute, 5233 Villigen PSI, Switzerland

<sup>2</sup>Delft University of Technology, Van der Maasweg 9, 2629 HZ Delft, The Netherlands

**Abstract** - heat exchanger tubes in bubbling fluidized bed reactors are necessary to remove the reaction heat of exothermal reactions. Vertical internals that mimic the heat exchanger tubes in cold-flow models, proofed to reduce the bubble size and lead to a more even distribution of the bubbles above the cross-section. Another option is to orientate the internals horizontally inside the column. By means of a measurement campaign at a cold-flow model, differences concerning the hydrodynamic behavior between a column with horizontal and vertical internals were investigated and determined. It turned out that the horizontal internals influence the hydrodynamics in a way which is not beneficial concerning the reactor performance due to an accumulation of bubbles below the horizontal internals and preferential pathways of the bubbles between the horizontal internals.

### 1. Introduction

Bubbling fluidized beds (BFB) are used in various industrial applications due to their high rates of heat and mass transfer (Kunii and Levenspiel, 2013). To control the temperature of highly exothermic reactions (e.g. methanation), the heat transfer area has to be enlarged by means of heat transfer tubes. The orientation of the heat exchanger tubes is commonly horizontal or vertical. The hydrodynamics around the immersed tubes greatly affect the heat transfer since the heat transfer coefficient is influenced by the mean contact time of particles with the tube surface as shown by (Chen, 2003). In a pseudo 2-D bubbling fluidized bed with horizontal internals, the bubble behavior was investigated by means of optical measurement techniques by (Asegehegn et al., 2011) and (Hull et al., 1999a). The solids mixing behavior of a bubbling fluidized bed was investigated in the scope of (Hull et al., 2000). X-ray measurements have been used by (Maurer et al. 2015a) and (Maurer et al. 2015b) to investigate the hydrodynamics in a 3-D bubbling fluidized bed with and without vertical internals. The hydrodynamic behavior in a 3-D bed with a horizontal tube bundle was investigated on the basis of computer simulations in (Li et al., 2011) and on the basis of X-ray photography in (Yates et al., 1990). In the scope of this study, X-ray measurements were performed in to investigate the fluidization behavior of a cold-flow 3-D bubbling fluidized bed with a diameter of 22 cm which is immersed by horizontal tubes. The experimental results obtained from the column with horizontal internals are compared with a dataset from a fluidized bed of the same diameter without and with vertical internals. Based on this comparison, the applicability of the investigated internals configuration can be judged regarding a future utilization under reactive conditions.

### 2. Experimental Setup

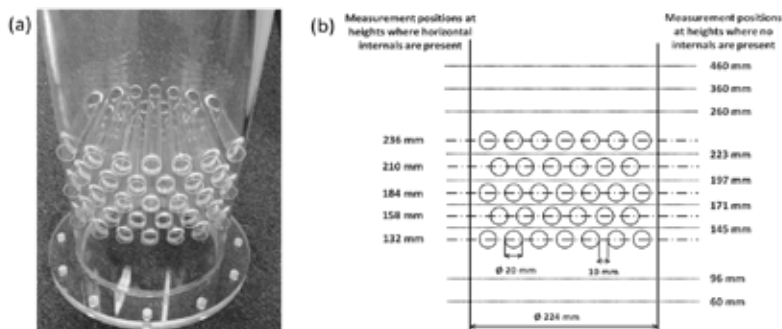


Fig. 1 (a) Picture of the column with horizontal internals; (b) schematic drawing of the horizontal internal location including the investigated measurement heights

The hydrodynamic experiments were conducted with a fast X-ray tomographic scanner located at TU Delft which is described in previous studies by (Mudde, 2011) and (Mudde et al., 2008). Alumina particles with a Sauter mean diameter of 289  $\mu\text{m}$  and a bulk density of 1350  $\text{kg/m}^3$  were used as bed material. The settled height of the non-fluidized bed is 50 cm. A detailed particle characterization is given by (Rüdisüli et al., 2012). Pressurized air was used to fluidize the particles and the volume flow was adjusted by a mass flow controller. The measurement campaign was conducted at room temperature and pressure. An acrylic glass cylinder with an inner diameter of 22 cm was used as the column. A picture of the empty column and a schematic side view of the horizontal internals including the investigated measurement heights and are shown in Fig. 1. The hollow horizontal tubes with an outer diameter of 20 mm were filled with bed material for the experiments. The horizontal spacing between the immersed tubes is 10 mm; the free space in the vertical direction is 6 mm.

The configuration of the applied X-ray tomographic setup is shown in Fig. 2. It consists of three X-ray point sources, arranged concentrically around the column with an angle of  $120^\circ$  between each source. The detection arrays are present at two heights with a vertical distance of 40 mm between them. The horizontal measurement plane consists of three detector arrays which are equipped with 32 single detectors, each. The upper detector array is located at the same height as the X-ray source and the average distance of the measurement planes inside the column is 18 mm. The attenuation of the X-ray beams at each detector is measured with a frequency of 2500 Hz to reconstruct the solid distribution of both measurement planes. Computation time was reduced by averaging 10 consecutive measurements resulting in an effective temporal resolution of 250 Hz. Each experimental setting was performed for 2 minutes to capture the entire bubble size or bubble rise velocity distribution for a statistically profound amount of data. Details about the reconstruction mechanism for the fast X-ray scanner are given in (Mudde, 2011). The reconstructed images can, for example, be used to determine the bubble size, the bubble rise velocity (BRV) or the hold-up distribution as shown in (Maurer et al., 2015b) and (Maurer et al., 2016).

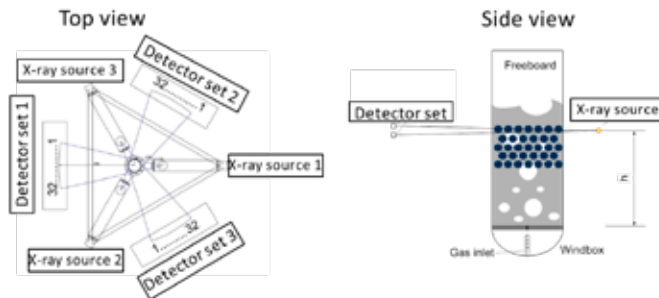


Fig. 2 Top view and side view of the X-ray tomographic setup adapted from (Maurer, et al., 2015b)

The time-averaged voidage distribution and the positions of the bubble centroids could be reconstructed for measurement heights between 13.2 cm and 23.6 cm since only the upper detector array is necessary to obtain this information. It should be pointed out that great caution was taken to ensure that the X-ray sources lie exactly in the same vertical plane like the upper detector array as depicted in Fig. 3.

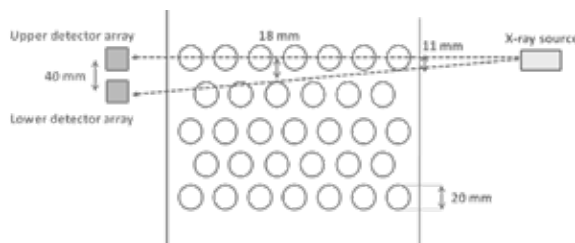


Fig. 3 Illustration of different penetrated geometries for X-ray beams detected by both detector arrays

For the investigated configuration with horizontal internals, the bubble rise velocity and the bubble size cannot be determined between the lowest and the highest horizontal tube due to geometrical constraints of the investigated configuration. This is based on the fact that the X-ray beams that reach the lower detector array do not cross the same geometry of the column as the X-ray beams reaching the upper detector array. This constriction is illustrated in Fig. 3 and would result in wrongly linked bubble events for which reason the size and the velocity of the bubbles will not be determined. For measurements with vertical internals, this constriction is negligible since the penetrated geometry of the X-ray beams is almost independent of the measurement height so this procedure could be used to determine the bubble size and bubble rise velocity (Maurer et al., 2015a).

In the following section, the hydrodynamic measurement results obtained from the column with horizontal internals are compared with the results for a configuration with and without vertical internals. A schematic top-view of the investigated configurations is shown in Fig. 4. Note that in contrast to the horizontal internals, the vertical internals range from the top of the column down to a height of 3 cm above the gas distributor.

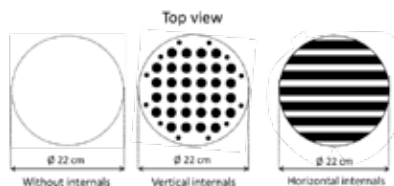


Fig. 4 Schematic top-view of all investigated internals configurations

### 3. Experimental Results

The bubble size plays an important role in the design of bubbling fluidized bed reactors since it influences parameters such as the gas or heat exchange between the bubble and the dense phase, the particle circulation rate or the elutriation of fine materials (Horio and Nonaka, 1987). In literature, a various number of bubble size correlations exists, but they are often restricted within the framework of defined experimental conditions as published by (Mori and Wen, 1975) and (Karimipour and Pugsley, 2011). The volume equivalent spherical bubble diameter  $d_{b,eq}$  is often used to characterize the bubble size and to derive correlations for the bubble rise velocity. It is defined based on the bubble volume  $V_b$  as:

$$d_{b,eq} = \left( \frac{6 V_b}{\pi} \right)^{1/3} \quad (1)$$

#### 3.1 Horizontal internals – Bubble size

For the configuration with horizontal internals, the number-weighted mean volume equivalent bubble diameter in dependence of the measurement height for the investigated fluidization numbers of 1.5, 2, 3 and 4 is shown in Fig. 5. As expected, the volume equivalent bubble diameter principally grows with an increasing measurement height and fluidization number. However, it is remarkable that for a fluidization number of 4, the bubble size of the measurement point below the region where the horizontal internals are located seems to fall out of the general pattern of results since the bubble size increases sharply. This apparent outlier could be explained with the constriction of the free cross-section at the height, where the horizontal internals begin. The flow resistance of the horizontal internals could lead to an accumulation of bubbles below this region and result in a larger effective bubble size for higher fluidization numbers. This effect does not seem to play a role if the fluidization number is low enough so that the bubbles may pass the section with horizontal internals without accumulating below this region. The significant increase of the bubble size for a fluidization number of four in the region below the immersed horizontal tubes has also been shown by means of a digital image analysis in a 2-D bed by (Asegehegn et al., 2011).

Except for a fluidization number of 4, the bubble size does not change significantly along the region where the horizontal internals are located. This may be due to the fact that the internals impede the bubble coalescence which is the reason of the bubble growth. For a fluidization number of 4, the decrease of the bubble size along the section with the horizontal internals may be due to the fact that the internals split the

larger bubbles that have accumulated below this region. In the region above the horizontal internals, the bubble size grows rapidly for all fluidization numbers as already shown in other studies that investigated the bubble size without internals (Glicksman et al., 1987) and (Maurer et al., 2015a).

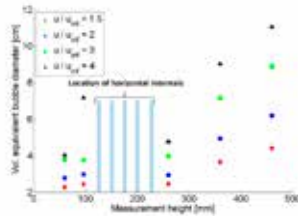


Fig. 5 Influence of  $u/u_{mf}$  on the mean volume equivalent bubble diameter for horizontal internals

### 3.2 Horizontal internals - Bubble Rise velocity

The bubble rise velocity is a major factor with regard to the conversion rate of a bubbling fluidized bed reactor especially for the case that the mass transfer between the bubble phase and the dense phase is the limiting step of the reaction. If the bubbles are fast and at the same time large, the risk of a breakthrough of reactants occurs. Fig. 6 shows the mean bubble rise velocity in dependency of the measurement height for fluidization numbers of 1.5, 2, 3 and 4 to analyze the influence of the horizontal internals on the bubble rise velocity. For fluidization numbers of 1.5 and 2 the bubble rise velocity increases below the horizontal internals and above the horizontal internals up to a measurement height of 260 mm. However, the reason for a transient slowdown of the bubble rise velocity at a height of 360 mm cannot be explained. The bubble rise velocity shows a different trend for fluidization numbers of 3 and 4. For these settings, the bubble rise velocity is almost constant below the region where the horizontal internals are located. This deviating trend could be explained that due to the bubble accumulation in the region below the horizontal internals the bubbles may not accelerate in the wake of other bubbles. Above the horizontal internals the bubble rise velocity increases steadily, as expected.

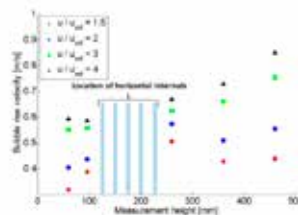


Fig. 6 Influence of  $u/u_{mf}$  on the mean bubble rise velocity for horizontal internals

### 3.3 Horizontal internals: Voidage distribution

Information about the voidage distribution is important for the performance of catalytic fluidized beds since it influences for example the internal heat distribution or the particle mixing inside the reactor. (Kopyscinski et al., 2009) have shown that in a BFB methanation reactor the catalyst bed material is regenerated internally due to circulation into the upper regions of the bed. The present X-ray measurements can be used to determine the time averaged bubble hold-up distribution above the cross-section of the column.

Fig. 7 shows the time-averaged voidage distribution at all investigated measurement heights for fluidization numbers of two, three and four. The average voidage is defined by the time a bubble is present at the particular position in the column divided by the total measurement time. For all heights, the voidage distribution is evaluated based on the data detected at the upper detector array. At the measurement heights where the horizontal internals are present, it should be pointed out that the X-ray beams that reach the upper X-ray detector array penetrate the horizontal internals at their full diameter as shown in Fig. 3. The given fluidization number refers to the cross-section without internals for which reason the actual fluidization number at the heights where the horizontal internals are present is higher.

The fact that for a fluidization number of 2 no bubbles accumulate below the horizontal internals is shown by the voidage distribution depicted in Fig. 7. Furthermore, the significantly larger bubble size for a fluidization number of 4 at a measurement height of 96 mm (see Fig. 5) is confirmed by the increased average voidage for this setting. Regarding the measurement heights where the horizontal internals are present, it turned out that even for a  $u/u_{mf}$  of two there are regions with an average voidage that is close to one. In areas with a high local average voidage, bubbles are present for most of the time. Whereas, only a few bubbles were detected above wide regions between the internals. Preferential pathways occur due to the inhomogeneous voidage distribution with the consequence that the particle mixing along in the entire column is not very pronounced. For fluidization numbers of three and four, the zones with an average voidage close to one may spread up to the entire length of the free space between the internals as it is visible in Fig. 7 for a fluidization number of four at measurement heights of 132 mm or 184 mm. However, even for these measurement points there are zones in which no bubbles are present.

The heat transfer in a fluidized bed depends among other factors on the contact between the particles and the heat transfer surfaces as shown by (Mickley and Fairbanks, 1955) and (Baskakov et al., 1973). Regarding the results of the voidage distribution at the heights where the horizontal internals are located, it has to be stated that the investigated internal configuration is not favorable for a good heat transfer. This is due to the fact that a lot of tubes are surrounded by voidage for most of the time which does not enable high heat transfer rates to the corresponding surfaces. Furthermore, this configuration does not support a good particle mixing since the majority of the free space between the internals shows a high voidage with the consequence that there is almost no exchange of bed material through these areas.

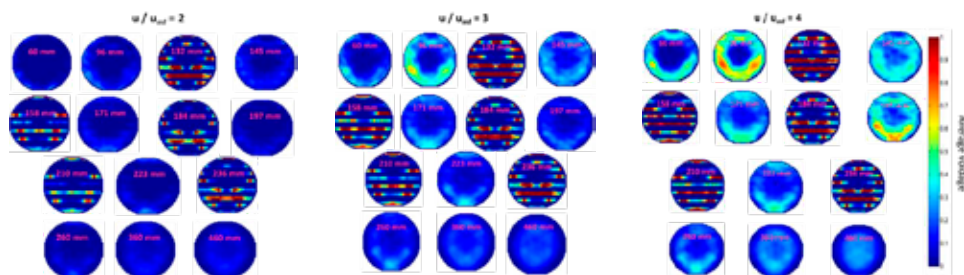


Fig. 7 Voidage distribution for  $u/u_{mf}$  of 2; 3 and 4 (The fluidization number refers to the cross-section without internals)

One possibility to achieve a better voidage distribution could be an increase of the free space between the horizontal internals which was only 10 mm in the horizontal direction for the investigated tube configuration. Investigations on two dimensional fluidized beds with immersed horizontal tubes and a larger distance between the single horizontal internals were conducted by (Asegehegn et al., 2011) and (Hull et al., 1999b), however, without presenting a voidage distribution. For all measurement heights that lie between two planes of horizontal internals, the increased free cross-sectional area leads to significantly lower average voidage values. For example, at a measurement height of 145 mm and a fluidization number of four the maximum voidage is roughly 0.4. At the measurement heights above the horizontal internals, the region with a slightly higher voidage has a circular shape around the center of the column that closes with increasing measurement height. The closing of the region with a higher hold-up has already been reported for a 14 cm  $\varnothing$  column without internals for the same bed material in (Maurer et al., 2015b).

### 3.4 Influence of internals orientation on the bubble rise velocity

The presence of internals in a bubbling fluidized bed has a great influence on the hydrodynamic behavior as it has already been shown for vertical internals by experiments on a  $\varnothing$  14 cm column in (Maurer et al., 2015a) and (Maurer et al., 2015b) as well as for horizontal internals based on a computer simulation in (Li et al., 2011). The influence of the different internal configurations (see Fig. 4) on the bubble properties is investigated in the scope of this study. The mean bubble rise velocity for fluidization numbers of two and four is shown in Fig. 8. The region where the horizontal internals are located for the corresponding configuration is again indicated in the following figures.

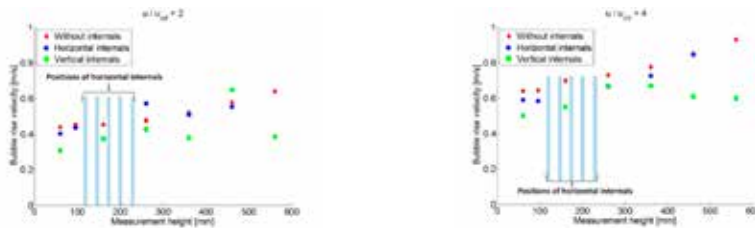


Fig. 8 Influence of internal orientation on the mean bubble rise velocity for  $u/u_{mf}$  of 2 and 4

For a fluidization number of two, the configuration without internals shows the highest bubble rise velocities up to a measurement height of 200 mm. For the horizontal internal configuration, the increase of the bubble rise velocity between 100 mm and 250 mm is more pronounced compared to the other configurations. The horizontal internals downstream seem to accelerate the bubbles upstream of the horizontal internals for a fluidization number of two. Above a measurement height of 360 mm, the difference in the bubble rise velocity between the configuration without internals and the configuration with horizontal internals is marginal. This finding could be interpreted in a way that the flow structure is influenced up to a maximum length of 120 mm above the horizontal internals. Except for a measurement height of 460 mm, the configuration with vertical internals leads to a lower bubble rise velocity compared to the configuration without internals as already shown for a smaller column in (Maurer et al., 2015a). Outlier at this measurement height could be explained by the fact that the local flow structure is disturbed by a spacer which is located slightly below a height of 460 mm to keep the internals at the intended position.

For a fluidization number of four, the configuration without internals generally resulted in the highest bubble rise velocity. Above the region where the horizontal internals are located, the BRV approaches again the values for the configuration without internals. However, the distance above the horizontal internals to reach an almost identical BRV like the configuration without internals is larger compared to a fluidization number of two. The configuration of vertical internals shows a maximum bubble rise velocity of approximately 0.65 m/s in the region between 260 mm and 360 mm before the bubbles slow down towards a measurement height of 460 mm. The finding that the BRV passes through a maximum if vertical internals are present has already been reported in (Maurer et al., 2015a).

### 3.5 Influence of internals orientation on the bubble size

The size of bubbles is influenced by many factors such as the column diameter, the fluidization number, the initial bubble size above the gas distributor, the particle size or the measurement height as shown by (Mori and Wen, 1975). In the scope of this study, the influence of the internal presence and their orientation inside the column on the bubble size is investigated. In Fig. 9, the volume equivalent bubble diameter is plotted in dependence of the measurement height for the investigated internal configurations. For a fluidization number of two, the bubble size only changes marginally along the section where the horizontal internals are located as already discussed in section 3.1. Whereas, bubbles are significantly larger below the horizontal internals compared to the measurement position above the internals for a fluidization number of four. Along the region where the horizontal internals are located, a mechanism of a continuous bubble splitting and coalescence was stated by (Asegehegn et al., 2011) that eventually leads to smaller bubbles. Due to the fact that the bubbles become smaller along the region where the internals are present, it could be shown that this mechanism probably also takes place in three-dimensional beds.

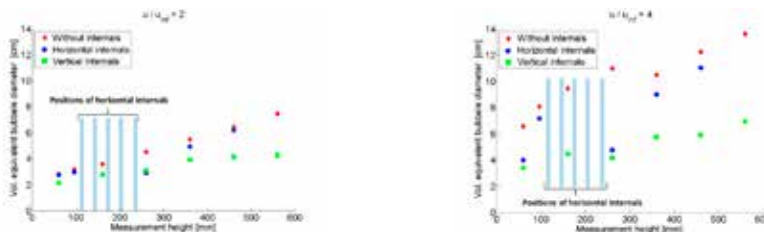


Fig. 9 Influence of internals orientation on mean volume equivalent bubble diameter for  $u/u_{mf}$  of 2 and 4

Analog to the trend of the bubble rise velocity for the horizontal configuration, the bubble size approaches the values of the configuration without internals for measurement heights above 260 mm. Again, this approach occurs faster for a fluidization number of two compared to a fluidization number of four. As expected and already shown for a column with a diameter of 14 cm in (Maurer et al., 2015a), the vertical internals have the effect to reduce the bubble diameter compared to the configuration without internals.

Another possibility to describe the bubble size is the hydraulic bubble diameter  $d_{b,hyd}$ , which is often used to calculate the heat and mass transfer in bubbling fluidized beds. It is defined based on the cross-sectional area  $S_b$  and the perimeter  $p_{er}$  determined for the horizontal plane that intersects the bubble centroid:

$$d_{b,hyd} = \frac{4 S_b}{p_{er}} \quad (2)$$

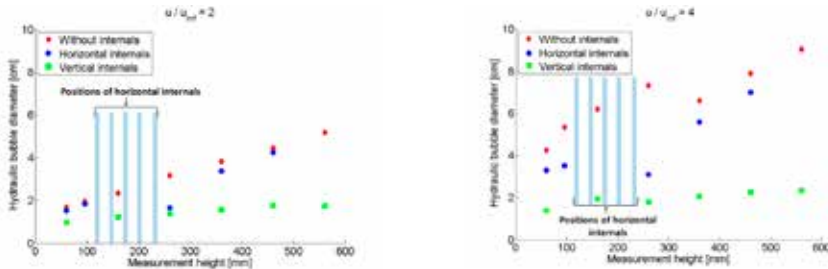


Fig. 10 Influence of internals orientation on mean hydraulic bubble diameter for  $u/u_{mf}$  of 2 and 4

Fig. 10 shows the mean number weighted hydraulic diameter for fluidization numbers of two and four. In general, the hydraulic diameter for the configuration with vertical internals shows the smallest values and is almost independent of the measurement position and the fluidization number. Similar findings have already been reported in the scope of (Maurer et al., 2015a) and can be regarded as favorable for the scale-up process of a bubbling fluidized bed reactor since the hydraulic bubble diameter which is a decisive factor for the mass transfer proved to be quite insensitive. Along the zone where the horizontal internals are located, the hydraulic bubble diameter also remains practically unchanged. However, in contrast to the volume equivalent diameter shown in Fig. 9, the hydraulic diameter does not increase significantly below the section of the horizontal internals. Above the region where the horizontal internals are located, the hydraulic diameter approaches the measurement values for the configuration without internals as it was already shown for the bubble rise velocity and the volume equivalent bubble diameter in the previous sections.

## 4. CONCLUSIONS

In the scope of this study, the influence of the internals orientation on the hydrodynamic behavior in bubbling fluidized beds was investigated. An X-ray tomographic scanner was used to conduct the measurements at a cold-flow bubbling fluidized bed with a diameter of 22 cm and immersed horizontal internals that are located at a column height between 13 cm and 23 cm to mimic the heat exchanger tubes. The results are compared with X-ray measurements that were performed at a bubbling fluidized bed for a configuration with vertical and without internals.

The fluidization behavior of the column with the horizontal internals proved to be critical. Even for lower fluidization numbers, it turned out that areas with a locally high voidage were detected at the measurement heights where the horizontal internals are located. For higher fluidization numbers, the zones of a very high voidage enlarged up to almost the entire free space between the horizontal internals. These findings are not favorable with regards to a good heat transfer since the particle mixing is not very pronounced. A larger distance between the horizontal tubes could lead to a more uniform distribution of voidage between the horizontal internals to improve both the particle mixing and the heat transfer. The comparison between the investigated internal configurations has shown that the hydraulic and the volume equivalent bubble diameter as well as the bubble rise velocity are in general the lowest for the configuration with vertical internals. In particular, the hydraulic bubble diameter which is an important parameter for the heat and mass transfer is almost independent of the measurement height for the configuration with vertical internals. In addition to a more homogeneous distribution of voidage, these findings facilitate the scale-up process if vertical internals are present compared to horizontal internals. Above the section where the horizontal internals are located, the

bubble properties approach the values of the configuration without internals earlier for lower fluidization numbers compared to higher fluidization numbers. This could be traced back to the fact that the flow pattern above the horizontal internals is less disturbed for lower fluidization numbers. The results of this study can be applied to judge the influence of the internal orientation on the hydrodynamic behavior of a bubbling fluidized bed and to reconsider the geometrical arrangement of horizontal internal tubes in fluidized beds to enable a better particle mixing between the lower and higher regions of the column.

## REFERENCES

- Asegehegn, T.W., Schreiber, M., Krautz, H.J., 2011. Investigation of bubble behavior in fluidized beds with and without immersed horizontal tubes using a digital image analysis technique. *Powder Technology* 210, 248–260.
- Baskakov, A.P., Berg, B.V., Vitt, O.K., Filippovsky, N.F., Kirakosyan, V.A., Goldobin, J.M., Maskaev, V.K., 1973. Heat transfer to objects immersed in fluidized beds. *Powder Technology* 8, 273–282.
- Chen, J.C., 2003. Surface contact - its significance for multiphase heat transfer: diverse examples. *Journal of heat transfer* 125, 549–566.
- Glicksman, L.R., Lord, W.K., Sakagami, M., 1987. Bubble properties in large-particle fluidized beds. *Chem. Eng. Sci.* 42, 479–491.
- Horio, M., Nonaka, A., 1987. A generalized bubble diameter correlation for gas-solid fluidized beds. *AIChE Journal* 33, 1865–1872.
- Hull, A.S., Chen, Z., Agarwal, P.K., 2000. Influence of horizontal tube banks on the behavior of bubbling fluidized beds: 2. Mixing of solids. *Powder Technology* 111, 192–199.
- Hull, A.S., Chen, Z., Fritz, J.W., Agarwal, P.K., 1999a. Influence of horizontal tube banks on the behavior of bubbling fluidized beds: 1. Bubble hydrodynamics. *Powder Technology* 103, 230–242.
- Hull, A.S., Chen, Z., Fritz, J.W., Agarwal, P.K., 1999b. Influence of horizontal tube banks on the behavior of bubbling fluidized beds: 1. Bubble hydrodynamics. *Powder Technology* 103, 230–242.
- Karimipour, S., Pugsley, T., 2011. A critical evaluation of literature correlations for predicting bubble size and velocity in gas-solid fluidized beds. *Powder Technology* 205, 1–14.
- Kopyscinski, J., Schildhauer, T.J., Biollaz, S.M.A., 2009. Employing Catalyst Fluidization to Enable Carbon Management in the Synthetic Natural Gas Production from Biomass. *Chemical Engineering & Technology* 32, 343–347.
- Kunii, D., Levenspiel, O., 2013. *Fluidization engineering*. Elsevier.
- Li, T., Dietiker, J.-F., Zhang, Y., Shahnam, M., 2011. Cartesian grid simulations of bubbling fluidized beds with a horizontal tube bundle. *Chemical Engineering Science* 66, 6220–6231.
- Maurer, S., Gschwend, D., Wagner, E.C., Schildhauer, T.J., Ommen, J.R. van, Biollaz, S.M.A., Mudde, R.F., 2016. Correlating bubble size and velocity distribution in bubbling fluidized bed based on X-ray tomography. *Chemical Engineering Journal*.
- Maurer, S., Wagner, E.C., Ommen, J.R. van, Schildhauer, T.J., Teske, S.L., Biollaz, S.M.A., Wokaun, A., Mudde, R.F., 2015a. Influence of vertical internals on a bubbling fluidized bed characterized by X-ray tomography. *Int. J. Multiphase Flow* 75, 237–249.
- Maurer, S., Wagner, E.C., Schildhauer, T.J., Ommen, J.R. van, Biollaz, S.M.A., Mudde, R.F., 2015b. X-ray measurements of bubble hold-up in fluidized beds with and without vertical internals. *International Journal of Multiphase Flow* 74, 118–124.
- Mickley, H.S., Fairbanks, D.F., 1955. Mechanism of heat transfer to fluidized beds. *AIChE Journal* 1, 374–384.
- Mori, S., Wen, C.Y., 1975. Estimation of bubble diameter in gaseous fluidized beds. *AIChE Journal* 21, 109–115.
- Mudde, R.F., 2011. Bubbles in a fluidized bed: A fast X-ray scanner. *AIChE J.* 57, 2684–2690.
- Mudde, R.F., Alles, J., Hagen, T.H.J.J. van der, 2008. Feasibility study of a time-resolving x-ray tomographic system. *Measurement Science and Technology* 19, 085501.
- Rüdisüli, M., Schildhauer, T.J., Biollaz, S.M.A., Ommen, J.R. van, 2012. Bubble characterization in a fluidized bed by means of optical probes. *Int. J. Multiphase Flow* 41, 56–67.
- Yates, J.G., Ruiz-Martinez, R.S., Cheesman, D.J., 1990. Prediction of bubble size in a fluidized bed containing horizontal tubes. *Chemical Engineering Science* 45, 1105–1111.